**Structure of siRNA.**

The followingsiRNAswere used simultaneously toknock down STC1 and UCP2:ID12722 for STC1:Forward,GGGAAAAGCAUUCGUCAAAtt;Reverse,UUUGACGAAUGCUUU UCCCtg;ID12905 for STC1:Forward,GGUCUAACUGUGGAAUAUAtt;Reverse,UAUAUUCCACAGUUA GACCtt;ID138790 for STC1:Forward,CGACUAACCUAUCUAUGAAtt;Reverse,UUCAUAGAUAGGUUA GUCGtt; IDs14630 for UCP2:Foreward,GCUAAAGUCCGGUUACAGAtt;Reverse,UCUGUAACCGGACUU UAGCag.AllsiRNAs were purchased from Ambion.

**XF-24 Oxygen Consumption Rate(OCR) and Extracellular Acidification Rate (ECAR)Measurements in detail.**

Thirty thousand($3x10^4$) A549 cells were seeded into each well of an XF24-well microplate (Seahorse Bioscience) and incubated for 16 hr under normal culture conditions.Prior to the experiment, the media was changed to assay medium (low-buffered RPMI 1640 containing 1 mM phosphate) and allowed to equilibrate for 1 hr. The plate was set in the machine, and baseline readings were obtained prior to

injection of compounds. Injected compounds included rSTC1 (final concentration 50ng/ml), or controls 2-deoxyglucose (2DG; final concentration 100mM; Sigma D6134) for inducing aerobic metabolism, (2R, 6aS, 12aS)-1,2,6,6a,12,12a-hexahydro-2-isopropenyl-8,9-dimethoxychromeno[3,4-b]furo[2,3-h]chromen-6-one, (Rotenon; final concentration 100nM; Sigma R8875) for inducing anaerobic metabolism and 2,4-dinitrophenol (2,4DNP; final concentration 100μM; Sigma D198501) for uncoupling oxidative phosphorylation.

**Supplemental Figures**

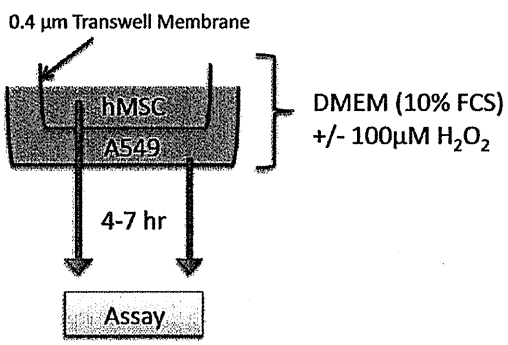


**Supplemental Figure 1.***Setup of the Co-culture Experiments.*MSCs were seeded at 1 × $10^3/cm^2$ on a cell-impermeable Transwell filter and A549 cells were seeded at 1 × $10^4/cm^2$ on a lower plate. The cells were cultured in Dulbecco's Modified Eagle's Medium (DMEM) containing 10% FBS with/without $H_2O_2$ (100 μM). Cell were harvested for viability assays after 7 hrs incubation, and after 4 hrs for biochemical assays.

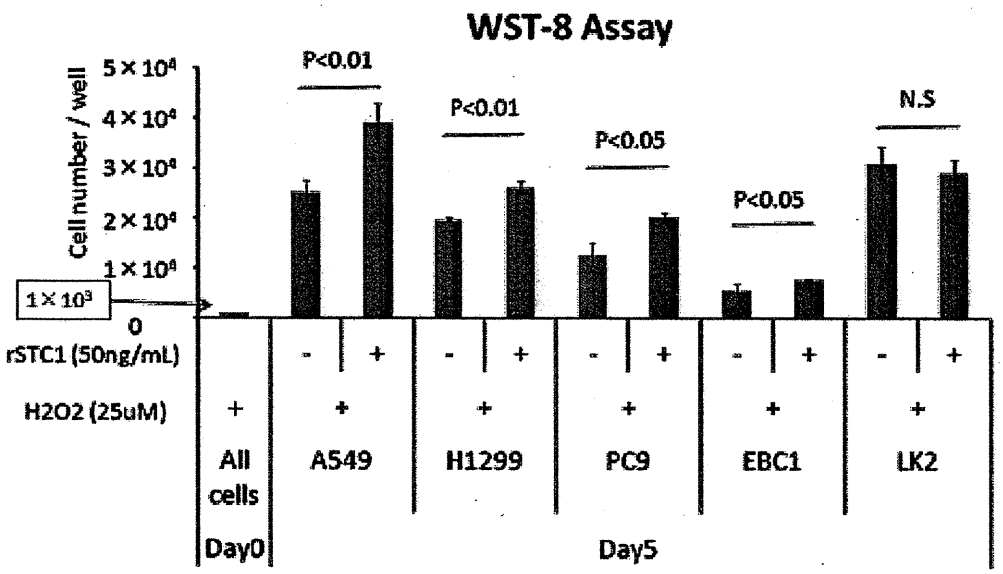


**Supplemental Figure 2.**r*STC1Promotes Survival in other Lung Epithelial Cell Linesafter 5-days*

Lung epithelial adenocarcinoma cell lines H1299, PC9 and lung epithelial squamous cancer cell lines EBC1, LK2 were cultured with $H_2O_2$ in the presence or absence of rSTC1 (50 ng/ml) and assayed for cell viability after 5-days in culture.

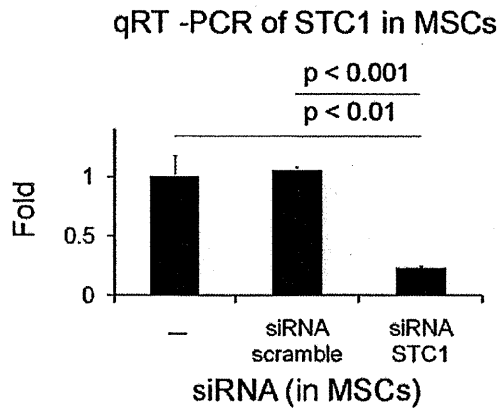


**Supplemental Figure 3.***Knockdown of STC1 in MSCs by siRNA.*MSCs were transfected with ansiRNA directed towards STC1. STC1 transcript levels were measured by real-time PCR.

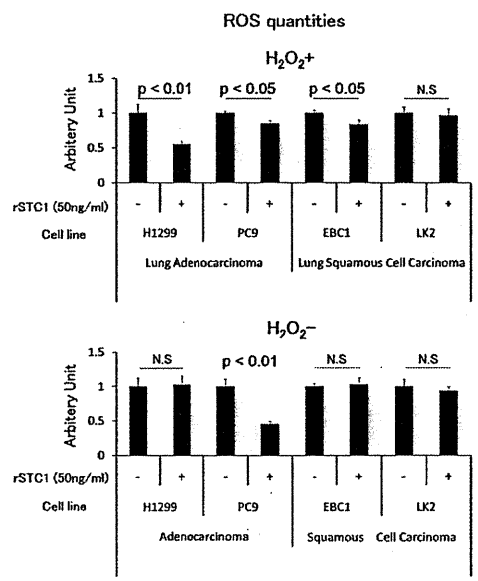


**Supplemental Figure 4.***Other Lung Epithelial Cells also Reduce ROS in Response to rSTC1.*Lung epithelial adenocarcinoma cell lines H1299, PC9 and lung epithelial squamous cancer cell lines EBC1, LK2 were cultured with or without $H_2O_2$ in the presence or absence of rSTC1 (50 ng/ml) and assayed for ROS production.

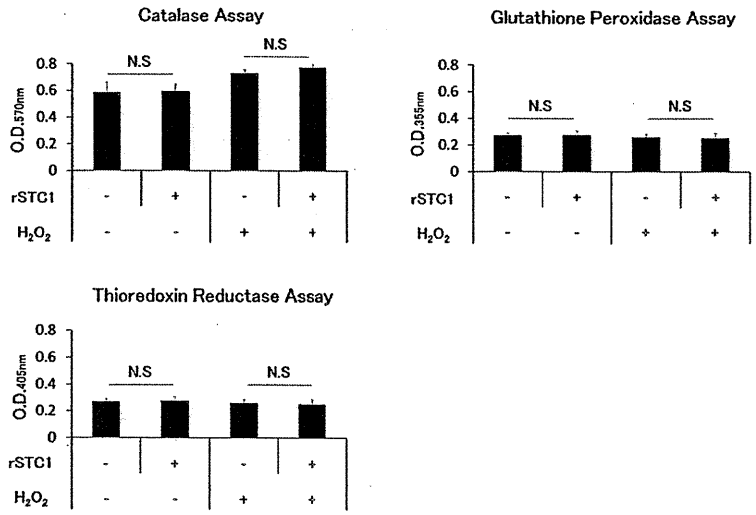


**Supplemental Figure 5.r*STC1 does not affect the activity of other canonical antioxidant enzymes.*** A549 cells were grown in the presence or absence of $H_2O_2$ (100 μM) with or without rSTC1 (50 ng/ml). Cells were assayed for Catalase, Glutathione Peroxidaseand ThioredoxinReductaseactivity .

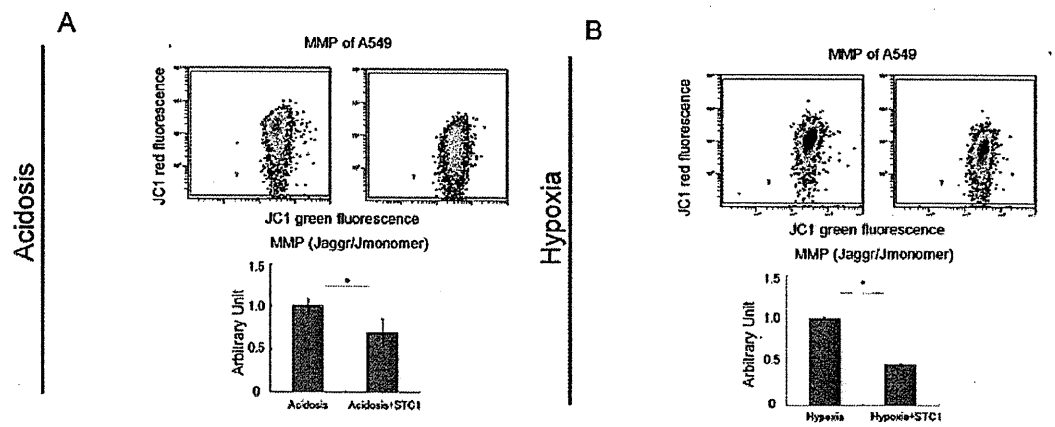


**Supplemental Figure 6.r*STC1reduces MMP in A549 Cells Grown in Hypoxia or Acidosis***

A549 cells were grown in hypoxia or acidosis with or without rSTC1 (50 ng/ml).

Cells were assayed for MMP by JC1 dye incorporation.

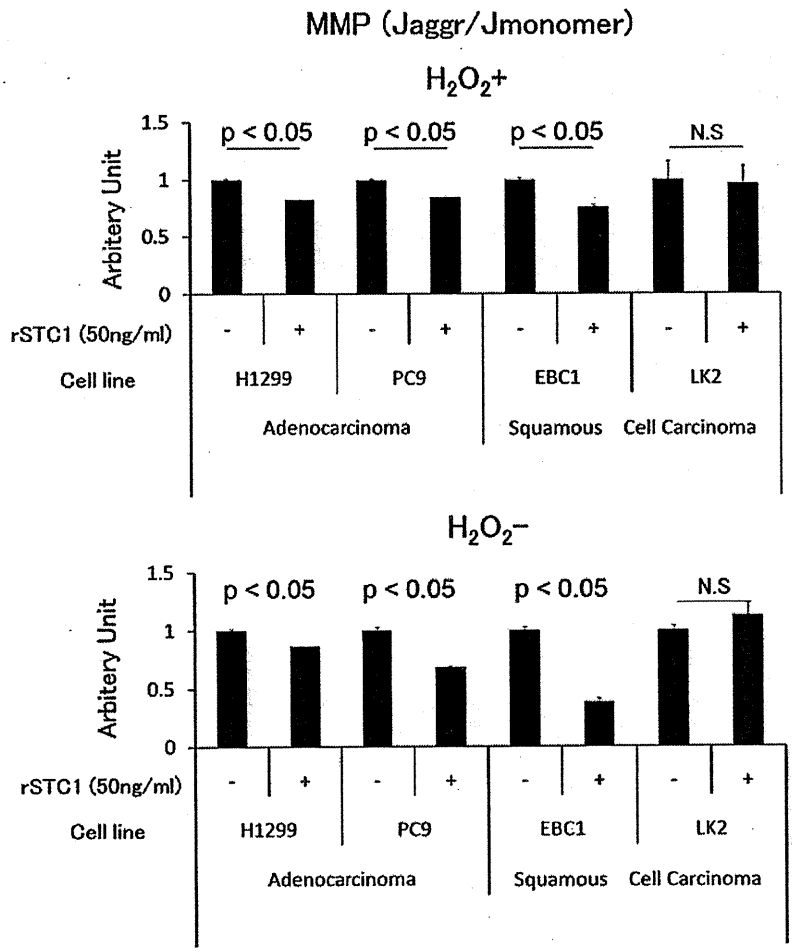


**Supplemental Figure 7.***rSTC1 reduced MMP in other Lung Epithelial Cell Lines*

Lung epithelial adenocarcinoma cell lines H1299, PC9 and lung epithelial squamous cancer cell lines EBC1, LK2 were cultured with or without $H_2O_2$ in the presence or absence of rSTC1 (50 ng/ml) and assayed for MMP by JC1 dye incorporation.

# Mesenchymal Stromal Cells Promote Tumor Growth through the Enhancement of Neovascularization

*Kazuhiro Suzuki,[1,2] Ruowen Sun,[1,3] Makoto Origuchi,[4] Masahiko Kanehira,[4] Takenori Takahata,[1] Jugoh Itoh,[1] Akihiro Umezawa,[5] Hiroshi Kijima,[6] Shinsaku Fukuda,[2] and Yasuo Saijo[1]*

[1]Department of Medical Oncology, Hirosaki University Graduate School of Medicine, Hirosaki, Japan; the [2]Department of Gastroenterology and Hematology, Hirosaki University Graduate School of Medicine, Hirosaki, Japan; the [3]Department of Rheumatology and Immunology, Shengjing Hospital of China Medical University, Shenyang, China; the [4]Department of Molecular Medicine, Tohoku University Graduate School of Medicine, Sendai, Japan; the [5]Department of Reproductive Biology, National Institute for Child Health and Development, Tokyo, Japan; and the [6]Department of Pathology and Bioscience, Hirosaki University Graduate School of Medicine, Hirosaki, Japan

Mesenchymal stromal cells (MSCs), also called mesenchymal stem cells, migrate and function as stromal cells in tumor tissues. The effects of MSCs on tumor growth are controversial. In this study, we showed that MSCs increase proliferation of tumor cells *in vitro* and promote tumor growth *in vivo*. We also further analyzed the mechanisms that underlie these effects. For use in *in vitro* and *in vivo* experiments, we established a bone marrow-derived mesenchymal stromal cell line from cells isolated in C57BL/6 mice. Effects of murine MSCs on tumor cell proliferation *in vitro* were analyzed in a coculture model with B16-LacZ cells. Both coculture with MSCs and treatment with MSC-conditioned media led to enhanced growth of B16-LacZ cells, although the magnitude of growth stimulation in cocultured cells was greater than that of cells treated with conditioned media. Co-injection of B16-LacZ cells and MSCs into syngeneic mice led to increased tumor size compared with injection of B16-LacZ cells alone. Identical experiments using Lewis lung carcinoma (LLC) cells instead of B16-LacZ cells yielded similar results. Consistent with a role for neovascularization in MSC-mediated tumor growth, tumor vessel area was greater in tumors resulting from co-injection of B16-LacZ cells or LLCs with MSCs than in tumors induced by injection of cancer cells alone. Co-injected MSCs directly supported the tumor vasculature by localizing close to vascular walls and by expressing an endothelial marker. Furthermore, secretion of leukemia inhibitory factor, macrophage colony-stimulating factor, macrophage inflammatory protein-2 and vascular endothelial growth factor was increased in cocultures of MSCs and B16-LacZ cells compared with B16-LacZ cells alone. Together, these results indicate that MSCs promote tumor growth both *in vitro* and *in vivo* and suggest that tumor promotion *in vivo* may be attributable in part to enhanced angiogenesis.



**Online address: http://www.molmed.org**
**doi: 10.2119/molmed.2010.00157**

## INTRODUCTION

Growth of solid tumors requires formation of the tumor stroma, which supplies oxygen and nutrients to tumor cells (1). The tumor stroma is composed of extracellular matrix and various mesenchymal cell types, including macrophages, endothelial cells, lymphocytes, pericytes, fibroblasts and myofibroblasts (2). These stromal cells communicate with tumor cells both through direct contact and through paracrine signaling mechanisms, mediated by secretion of soluble factors, including cytokines, chemokines and growth factors (3–7). Interactions between tumor cells and stromal cells regulate tumor growth, invasion, metastasis and angiogenesis (3–7). Among stromal cells, tumor-associated fibroblasts have been shown to be associated with increases in tumor growth and metastatic potential, leading to a poor prognosis (8,9). Tumor-associated fibroblasts and myofibroblasts originate from multiple sources and range from migratory neighboring cells to distant invading cells (10). Data from human tumors and mouse tumor models suggest that at least a portion of the stromal cells are derived from the bone marrow (11–13).

Mesenchymal stromal cells (MSCs), also called mesenchymal stem cells, are pluripotent progenitor cells that have the capability to differentiate into chondrocytes, adipocytes and osteoblasts, among other types of cells (14). Although MSCs primarily reside in the bone marrow (15), they are also found in adipose tissue, in the lungs and in many other organs, where they are involved in maintenance

***Address correspondence and reprint requests to*** *Yasuo Saijo, Department of Medical Oncology, Hirosaki University Graduate School of Medicine, 5 Zaifumacho, Hirosaki 036-8562, Japan. Phone: +81-172-39-5345; Fax: +81-172-39-5347; E-mail: yasosj@cc.hirosaki-u.ac.jp.*
*Submitted August 20, 2010; Accepted for publication March 10, 2011; Epub (www.molmed.org) ahead of print March 11, 2011.*

and regeneration of connective tissues (16). MSCs are known to migrate to tissues as a result of inflammation or injury, where they contribute to regeneration of the damaged tissues (17). For these reasons, MSCs have considerable therapeutic potential in tissue regeneration (18,19).

Recent results from both animal models and human tumors have suggested that MSCs also migrate to tumor tissues, where they incorporate into the tumor stroma (20,21). This tropism of MSCs for tumors is reportedly due to the presence of soluble factors secreted by tumor cells, similar to inflammatory responses (22,23). These findings have led to increased interest in understanding the effects of MSCs in the tumor microenvironment. Several studies have suggested that MSCs promote tumor growth and the metastatic potential of tumor cells (3,24). MSCs can differentiate into fibroblasts, myofibroblasts or pericyte-like cells and induce neoangiogenesis, resulting in the promotion of tumor growth *in vivo* (24,25). In contrast, few studies have indicated that MSCs inhibit tumor growth (26). Several studies have used human MSCs, as opposed to murine MSCs, to assess the effects of this cell type on tumor growth in mouse models because of the ease of expansion of human MSCs (3,24). In these tumor xenograft models, the tumor stroma consists of mouse cells, but the tumoral cells and MSCs are of human origin. Thus, because of the mixed lineages of these cells, the effects of MSCs on tumor growth may be affected by unknown interactions. On the basis of these previous studies, we elected to use only murine cells throughout the present study for the purpose of clearly interpreting the resulting findings.

In this study, we developed a quantitative assay for tumor growth *in vitro* using coculture models with MSCs and B16 melanoma cells expressing LacZ (B16-LacZ). We demonstrated that both direct contact with MSCs and release of soluble factors from MSCs promote B16-LacZ cancer cell proliferation *in vitro*. Furthermore, our results suggest that co-injection of MSCs with B16-LacZ cells promotes tumor formation in mice through enhanced angiogenesis, induced by secretion of proangiogenic factors from MSCs.

## MATERIALS AND METHODS

### Cell Culture and Animals

B16-LacZ, a mouse melanoma cell line expressing β-galactosidase, and TSt-4, a mouse MSC cell line derived from fetal thymus tissue (27), were obtained from the RIKEN BioResource Center (Tsukuba, Japan). B16-LacZ cells were cultured in Dulbecco's modified Eagle's medium (DMEM) supplemented with 10% fetal bovine serum (FBS; DMEM/10% FBS). Lewis lung carcinoma (LLC) cells were obtained from the Cell Resource Center for Biomedical Research, Tohoku University (Sendai, Japan). LLC cells were propagated in RPMI-1640 containing 10% FBS. A mouse bone marrow–derived mesenchymal cell line (MSC) was established from bone marrow cells isolated from C57BL/6 mice, as described previously (28). MSCs were cultured in DMEM low glucose 1× medium (DMEM + GlutaMAX; Invitrogen, San Diego, CA, USA) containing 10% FBS (Invitrogen). Female C57BL/6 mice, 6–8 wks of age, were purchased from Japan Charles River (Atsugi, Japan). Female C57BL/6-Tg (CAG-EGFP) Q1 mice were purchased from Japan SLC (Hamamatsu, Japan). For primary culture of MSCs from GFPQ2 mice, the bone marrow suspension was cultured in DMEM + GlutaMAX with 10% FBS. When adherent cells reached 70–80% confluence, cells were harvested and expanded. When a homogeneous cell population was obtained, after 3 to 5 passages, these cells were used for subsequent experiments.

### Analysis of MSC Cell Surface Markers

Cell surface antigens were analyzed by flow cytometry in cultured murine MSCs. Briefly, $1 \times 10^5$ cells were incubated with the following fluorescence-conjugated rat monoclonal antibodies: antimouse Sca-1 (Ly-6A/E; BD Pharmingen, San Diego, CA, USA), antimouse CD44 (Pgp-1/Ly-24; eBioscience, San Diego, CA, USA), antimouse CD34 (Beckman Coulter, Fullerton, CA, USA), antimouse CD45 Q6 (leukocyte common antigen) (Beckman Coulter) and antimouse CD90 (Thy-1; Beckman Coulter). Nonspecific fluorescence was assessed by incubation of cells with isotype-matched rat monoclonal antibodies (BD Pharmingen). Data were analyzed by collecting 20,000 events on a Cell Lab Quanta SC (Beckman Coulter).

### *In Vitro* Cell Proliferation Assays

For proliferation assays using cocultured cells, MSCs were seeded at $5.0 \times 10^3$ cells/well in 96-well plates in DMEM containing 1% FBS (DMEM/1% FBS). After 12 h, B16-LacZ cells were added ($5.0 \times 10^3$ cells/well) to cultured MSCs. After an additional 24 h, cells were fixed by incubation in phosphate-buffered saline (PBS) containing 5.4% formaldehyde and 0.8% glutaraldehyde at 12-h time points. After two washes with PBS, 100 μL 5-bromo-4-chloro-3-indolyl-β-D-galactopyranoside (X-Gal) solution (2 mg/mL) was added to each well. Cells were then incubated at 37°C in a humidified atmosphere containing 5% $CO_2$ in the dark for 12 h. Absorbance at 595 nm was measured using an E-Max precision microplate reader (Molecular Devices, Menlo Park, CA, USA).

For proliferation assays performed in the absence of direct contact between MSCs and B16-LacZ cells, MSCs were seeded at a density of $5.0 \times 10^4$ cells/well in 24-well plates in DMEM/1% FBS. After a 12-h incubation, wells were covered with Cell Disks (Sumitomo Bakelite, Tokyo, Japan) that serve as a bulkhead, and B16-LacZ cells ($5.0 \times 10^4$ cells/well) were added to the cell disks. After an additional 48 h, cells were lysed by the addition of lysis buffer (0.5% Triton X-100, 2 mol/L NaCl in PBS) at 12-h time points, and 100 μL 2 mg/mL X-Gal solution was combined with 15 μL of the cell suspension. The absorbance at 595 nm of the resulting solution was then measured as described above.

To assess cell proliferation in the presence of conditioned media from MSCs, media were collected from MSCs ($2 \times 10^6$ cells) cultured in 10 mL DMEM/1% FBS in a culture dish (10 cm in diameter) for 48 h. The media were clarified by centrifugation (1,000*g*, 5 min), and the resulting supernatant was used as conditioned media. B16-LacZ cells were seeded at a density of $5.0 \times 10^3$ cells/well in 96-well plates and cultured in DMEM/10% FBS for 12 h. Subsequently, the media were replaced with either conditioned media or DMEM/1% FBS. Next, 10 μL Alamar Blue assay solution (Biosource International, Camarillo, CA, USA) was added to the wells at 12-h time points, and the plates were incubated at 37°C. Fluorescence was measured using a Fluoroskan Ascent CF apparatus (Labsystems, Helsinki, Finland) with excitation set to 544 nm and emission set to 590 nm.

### Analysis of *In Vivo* Tumor Growth

All animal experiments were reviewed and approved by the Institutional Animal Care and Use Committee of Hirosaki University.

All mice (n = 8 for each group) were divided into groups that received subcutaneous injections of either (a) B16-LacZ cells alone ($5.0 \times 10^5$ cells), (b) B16-LacZ cells ($5.0 \times 10^5$ cells) with MSCs ($1 \times 10^5$ cells) at a 1:0.2 ratio, (c) B16-LacZ cells ($5.0 \times 10^5$ cells) with MSCs ($5.0 \times 10^5$ cells) at a 1:1 ratio, (d) B16-LacZ ($5.0 \times 10^5$ cells) with MSCs ($2.5 \times 10^6$ cells) at a 1:5 ratio or (e) MSCs alone ($2.5 \times 10^6$ cells). All cell suspensions were delivered in a final volume of 200 μL and injected subcutaneously into the right side of the abdomen. LLC cells were transplanted instead of B16-LacZ cells under identical conditions. Beginning 5 d after cell injections, the tumor volume was calculated every 2 d using the following formula: tumor volume ($mm^3$) = 0.52 × width $(mm)^2$ × length (mm).

### Immunohistochemistry of the Tumors

B16-LacZ tumors on day 21 were removed, fixed in 10% buffered formalin for 24 h and then stained with hematoxylin and eosin for histological examination. For immunohistochemical staining for Ki-67, sections were deparaffinized and antigen retrieval was conducted using an antigen retrieval solution (415211; Nichirei, Tokyo Japan). After blocking of endogenous peroxidase activity with a peroxidase blocking reagent (S2001; Dako, San Antonio, TX, USA), tissue sections were incubated with rat antimouse Ki-67 (1:25; Dako) and the appropriate secondary antibody. Color development was performed using the peroxidase substrate 3-amino-9-ethylcarbazole.

To characterize the effects of MSCs on microvessel area in tumor tissues, tumors were removed when the tumor size reached around 1 $cm^3$ or at day 21. Cryosections were fixed with 4% paraformaldehyde and stained with rat antimouse CD31 (1:100; BD Pharmingen). Sections were then incubated with labeled polymer (N-Histofine Simple Stain Mouse MAX PO [Rat]; Nichirei, Tokyo, Japan). Color development was performed using 3-amino-9-ethylcarbazole. Sections were counterstained with hematoxylin. Microvessel area in cryosections from each tumor was quantified using 10 images from each of 10 different tumors per group under 200× magnification. Vessel area was measured using the ImageJ software (http://rsbweb.nih.gov/ij).

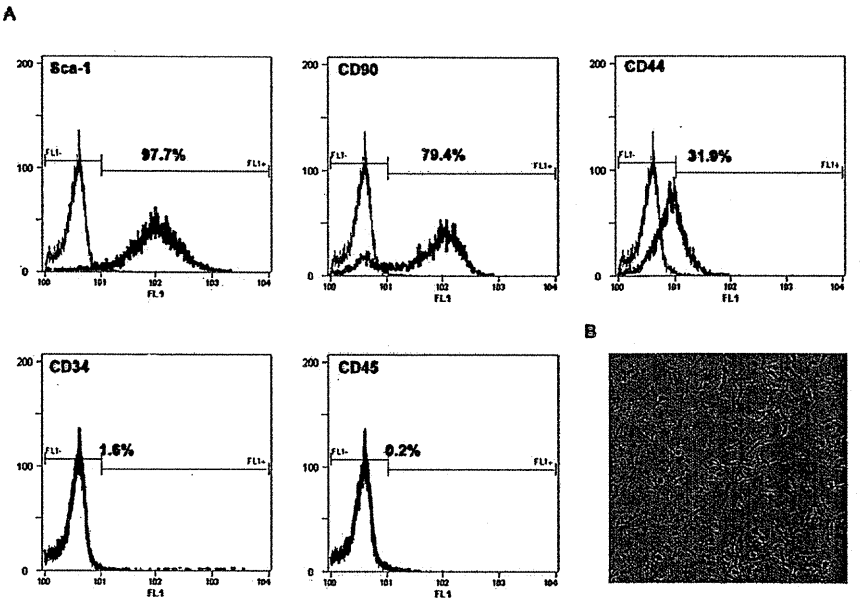


**Figure 1.** Flow cytometric and morphological analysis of MSCs. (A) Mouse bone marrow–derived MSCs established from cells obtained in C57BL/6 mice were stained with antibodies directed against Sca-1, CD90, CD44, CD34 and CD45 and were analyzed by flow cytometry. (B) Morphology of MSCs in culture.Q8

### Immunofluorescence

On day 21, B16-LacZ tumors with MSCs expressing GFP (GFP-MSCs) were fixed with 4% paraformaldehyde and increasing concentrations of sucrose buffer (12%, 15% and 18%) over 12 h. Frozen sections were blocked with Protein Block Serum-Free (X0909; Dako) and were incubated with rat antimouse CD31 (1:100; BD Pharmingen) or rabbit antimouse α smooth muscle actin (α-SMA, 1:50, ab5694; Abcam, Cambridge, U.K.). Rat $IgG_{2a}$ and rabbit IgG were used as isotype controls. Secondary antibodies used were donkey antirat IgG-Alexa Fluor 594 (1:200; Invitrogen) or goat antirabbit IgG-Alexa Fluor 594 (1:200; Invitrogen), respectively. To improve primary antibody penetration, sections for α-SMA staining were incubated in PBS/0.02% Triton

X-100 for 30 min at room temperature before primary antibody incubation. All procedures were protected from light. Sections were examined with a confocal laser scanning microscope.

### Analysis of Angiogenic Factor Levels in Supernatants from B16-LacZ Cells and MSCs

To measure the levels of angiogenic factors secreted by B16-LacZ cells and MSCs, B16-LacZ cells alone ($1.0 \times 10^6$ cells), MSCs alone ($1.0 \times 10^6$ cells) or both B16-LacZ cells and MSCs ($1.0 \times 10^6$ cells each) were cultured for 24 h in 10 mL DMEM/10% FBS media. The media were then collected and clarified by centrifugation (1,000*g*, 5 min), and the resulting supernatants were used for analysis. Concentrations of vascular endothelial growth factor (VEGF), macrophage inflammatory protein-2 (MIP-2; functional homolog of human interleukin [IL]-8), macrophage colony-stimulating factor (M-CSF), leukemia inhibitory factor (LIF), IL-15, IL-18, basic fibroblast growth factor (bFGF), monokine induced by interferon γ (MIG) and platelet-derived growth factor (PDGF) were determined with the Bio-Plex cytokine assay (Bio-Rad, Hercules, CA, USA) using a Luminex 200 (Luminex, Austin, TX, USA).

### Statistical Analysis

Results are expressed as the mean ± standard deviation (SD). Comparisons between groups were performed using a two-tailed Student *t* test. Linear regression curves were produced using the Pearson correlation. *P* values <0.05 indicated statistical significance.

## RESULTS

### *In Vitro*–Cultured Mesenchymal Cells Express MSC Markers

Mouse bone marrow–derived MSC cultures were established from bone marrow cells isolated in C57BL/6 mice. Phenotypically, MSCs were characterized by being negative for expression of the CD34 and CD45 hematopoietic cell markers and positive for Sca-1, CD90 and CD44. Flow cytometric analysis revealed that cultured MSCs were positive for Sca-1, CD90 and low expression of CD44, but negative for CD34 and CD45 (Figure 1A), as expected. The MSCs exhibited a spindle-shaped morphology in culture (Figure 1B) and have been reported to differentiate into adipocytes and osteocytes (28). These results were consistent with previous reports and indicated that the established cell line indeed consisted of MSCs (29).

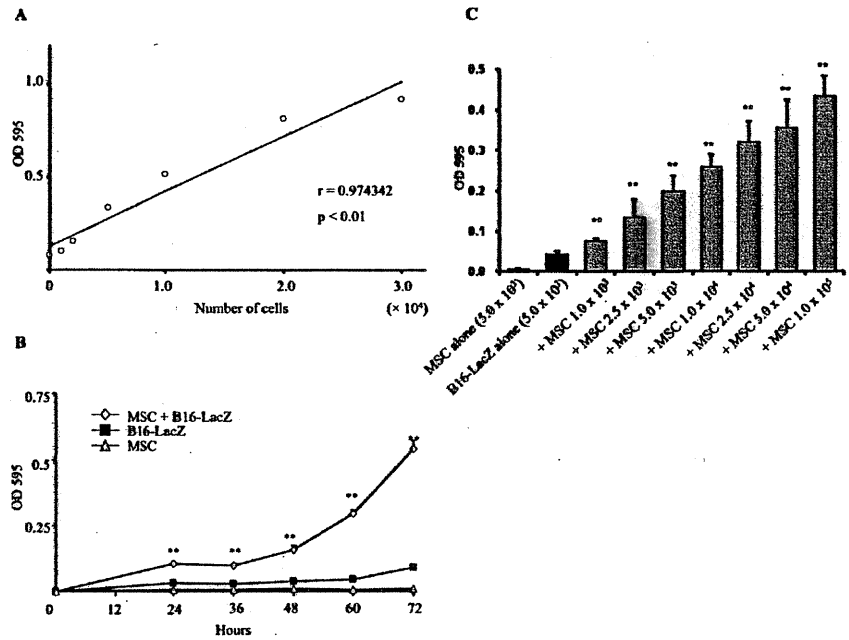


**Figure 2.** Proliferation of B16-LacZ cells cocultured with mesenchymal stromal cells (MSCs). (A) Standard curve correlating LacZ expression with cell numbers. B16-LacZ cells were seeded on 96-well plates at different cell numbers. After 24 h, β-galactosidase protein levels were analyzed in each well by measuring the absorbance at 595 nm using a microplate reader, as described in "Materials and Methods." (B) B16-LacZ cells were cultured with MSCs at a 1:1 ratio. β-Galactosidase protein expression was measured at the indicated time points (n = 5; $^{**}P < 0.01$). (C) B16-LacZ cells were incubated with MSCs at different ratios. β-Galactosidase protein expression was measured after 48 h (n = 8; $^{**}P < 0.01$).

### Coculture with MSCs Promotes Proliferation of B16-LacZ Cells *In Vitro*

We next analyzed whether MSCs could promote proliferation of the murine melanoma cell line B16-LacZ in an *in vitro* coculture model. Initially, a linear regression standard curve was generated to correlate the number of B16-LacZ cells with absorbance at 595 nm ($OD_{595}$). The assay was selective for B16-LacZ cells, because only this cell line expressed β-galactosidase (Figure 2A). Results from this analysis revealed that coculture of B16-LacZ cells with MSCs led to a marked increase in proliferation of B16-LacZ cells compared with B16-LacZ cells cultured alone (Figure 2B). After 48 h, the number of cells grown under coculture conditions was 3.6-fold greater than that of B16-LacZ cells cultured alone. On the basis of these results, we next analyzed the dose-response effect of MSCs on B16-LacZ proliferation (Figure 2C). These results showed that proliferation of B16-LacZ cells increased in accordance with the number of MSCs present in the coculture.

### MSCs Promote B16-LacZ Cell Proliferation in the Absence of Direct Contact

To determine whether direct contact between B16-LacZ cells and MSCs is re-

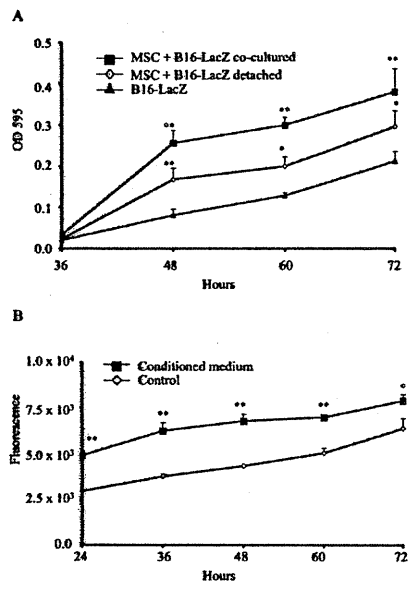


**Figure 3.** Effects of MSCs on B16-LacZ cell proliferation in the absence of direct contact. (A) B16-LacZ cells and MSCs were cultured together but were separated by a bulkhead consisting of a cell disk. Absorbance at 595 nm was determined at the indicated time points (n = 7; $^*P < 0.05$; $^{**}P < 0.01$). (B) B16-LacZ cells were cultured in conditioned medium from MSCs. Cell proliferation was measured using the Alamar Blue assay as described in the "Materials and Methods" (n = 7; $^*P < 0.05$; $^{**}P < 0.01$).

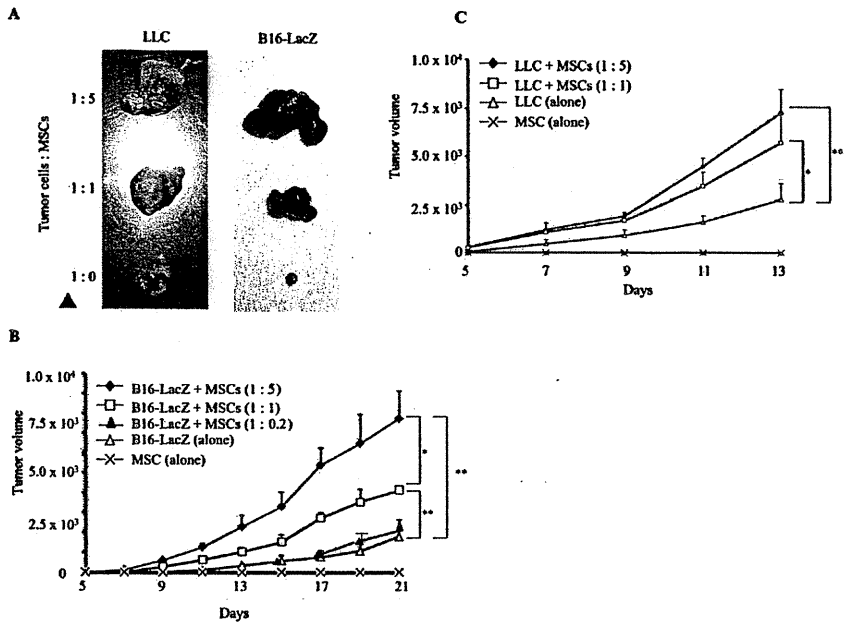


**Figure 4.** Analysis of tumors derived from xenografts of B16-LacZ cells or LLCs co-injected with MSCs. (A) Representative photographs of B16-LacZ tumors and LLC tumors. (B) B16-LacZ cells and MSCs were co-injected into the right side of the abdomen of C57BL/6 mice at a ratio of 1:0.2, 1:1 or 1:5. Tumor volume was calculated at 2-day intervals (n = 7; $^*P < 0.05$; $^{**}P < 0.01$). (C) LLCs and MSCs were co-injected as described for B16-LacZ cells, and tumor volume was calculated at 2-day intervals (n = 7; $^*P < 0.05$, $^{**}P < 0.01$).

quired for stimulation of B16-LacZ cell proliferation, cell growth in the absence of direct contact was investigated using cell disks and conditioned medium. Although the magnitude of stimulation of cell proliferation cannot be directly compared between cocultured cells and cells cultured in the absence of direct contact because of differences in growth conditions, a 2.3-fold increase in proliferation of B16-LacZ cells occurred in the presence of MSCs cultured on cell disks ($P < 0.01$; Figure 3A), and a 1.4-fold increase occurred in the presence of conditioned media ($P < 0.01$; Figure 3B) at 48 h. These values were slightly lower than the 6.4-fold increase in proliferation that occurred under conditions of 60-h direct contact in cocultures (see Figure 2B). To characterize the mechanisms underlying these changes in cell proliferation, we performed cell cycle analysis using flow cytometry. However, no obvious change in the cell cycle distributions of the cancer cells was apparent at the time points analyzed (data not shown).

### MSCs Derived from Bone Marrow Promote Tumor Growth *In Vivo*

B16-LacZ cells and LLC cells, a lung carcinoma cell line, were used to assess the effects of MSCs on tumor promotion and growth in an *in vivo* model. Mixtures containing each of these cell types, along with MSCs, at ratios of 1:0.2, 1:1 and 1:5, were subcutaneously injected into syngeneic C57BL/6 mice, and tumor formation and growth were assayed. At day 21 after tumor inoculation, mice injected with B16-LacZ cells and MSCs at 1:1 and 1:5 ratios exhibited 2.3-fold ($P < 0.01$) and 4.3-fold ($P < 0.01$) greater tumor volumes, respectively, than mice injected with B16-LacZ cells alone (Figure 4A, B). However, tumor ratio of 1:0.2 did not increase tumor size compared with B16-LacZ cells alone (see Figure 4B). At day 13 after tumor inoculation, mice injected with LLCs and MSCs at 1:1 and 1:5 ratios exhibited 2.1-fold ($P < 0.05$) and 2.6-fold ($P < 0.01$) greater tumor volumes, respectively, compared with mice injected with LLCs alone (Figure 4A, C). Injection of MSCs alone did not result in tumor formation. Mixtures of B16-LacZ cells and another MSC cell line, TSt-4, derived from fetal thymus tissue, were also injected into C57BL/6 mice to assess the tumor growth effect of MSCs from a different origin. However, we observed no stimulatory or inhibitory effect on B16-LacZ tumor growth by TSt-4 MSCs at 1:1 and 1:5 ratios (data not shown). To exclude the possibility that increased tumor growth was due to immunosuppression caused by MSCs, B16-LacZ cells and/or MSCs were subcutaneously injected into BALB/c nude mice. Similar to the re-

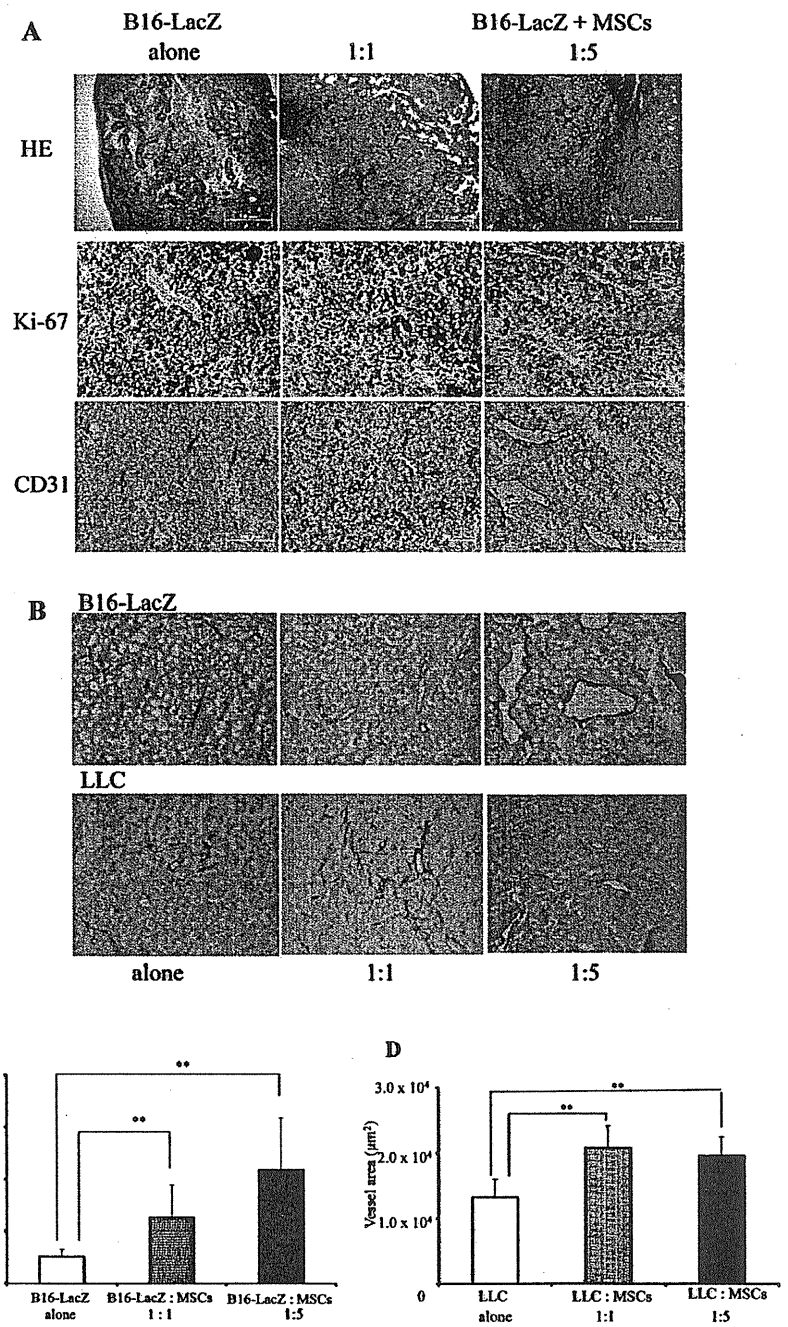


**Figure 5.** Analysis of B16-LacZ tumors in xenograft tumor models in the presence and absence of co-injected MSCs. (A) Photographs of tumors generated by injection of B16-LacZ alone or by co-injection of B16-LacZ cells with MSCs. On day 21, tumors were stained with hematoxylin and eosin, a Ki-67 antibody and a CD31 antibody. (B–D) Quantitative analyses of tumor angiogenesis. When tumors reached approximately 1 $cm^3$, they were removed, fixed and stained with a CD31 antibody (B). Microvessel density in tumor cryosections was analyzed by visualization of CD31 staining at 200× magnification. Microvessel density was quantified using the ImageJ software (n = 10; $^*P < 0.05$; $^{**}P < 0.01$). (C) B16-LacZ. (D) LLC.

Q7

sults described above for syngeneic mice, co-injection of B16-LacZ cells and MSCs caused a significant increase in tumor volume compared with injection of B16-LacZ cells alone in nude mice ($P < 0.05$; data not shown).

### MSCs Promote Tumor Growth *In Vivo* by Increasing Angiogenesis

To investigate mechanisms of tumor promotion by MSCs, we analyzed B16-LacZ + MSC tumors on day 21 (Figure 5). Hematoxylin and eosin staining revealed a massive necrotic area in B16-LacZ alone tumors, but not in B16-LacZ + MSC tumors (Figure 5A). *In vivo* analysis of cell proliferation using Ki-67 labeling was compared between B16-LacZ alone and B16-LacZ + MSC tumors (see Figure 5A). Percentages of Ki-67–positive cells in B16-LacZ alone tumors, B16-LacZ + MSC tumors at a 1:1 ratio and B16-LacZ + MSC tumors at a 1:5 ratio were 44.3 ± 5.1, 49.1 ± 3.4 and 42.4 ± 7.8, respectively, and were not significantly different. Thus, we hypothesized that MSCs may promote tumor growth by increasing angiogenesis. To assess whether MSCs promote angiogenesis, cryosections from tumors were stained with an antibody directed against CD31 to visualize blood vessels (see Figure 5A). Blood vessels were richer in B16-LacZ + MSC tumors (at ratios of 1:1 and 1:5) than in B16-LacZ alone tumors on day 21.

For optimal quantitative analysis of angiogenesis, we stained smaller tumors (around 1 $cm^3$) with CD31 antibody instead of large tumors on day 21. Blood vessel density was then analyzed by quantification of $CD31^+$ areas. Results from this analysis revealed that vessel area was increased in mice co-injected with B16-LacZ cells and MSCs (at ratios of 1:1 and 1:5) compared with mice injected with B16-LacZ cells alone ($P < 0.01$; Figure 5B, C). Similar results were observed when LLCs were used in place of B16-LacZ cells ($P < 0.01$). However, no significant difference was observed in mice co-injected with different ratios of cancer cells to MSCs (1:1 and 1:5, respectively; Figure 5B, D).

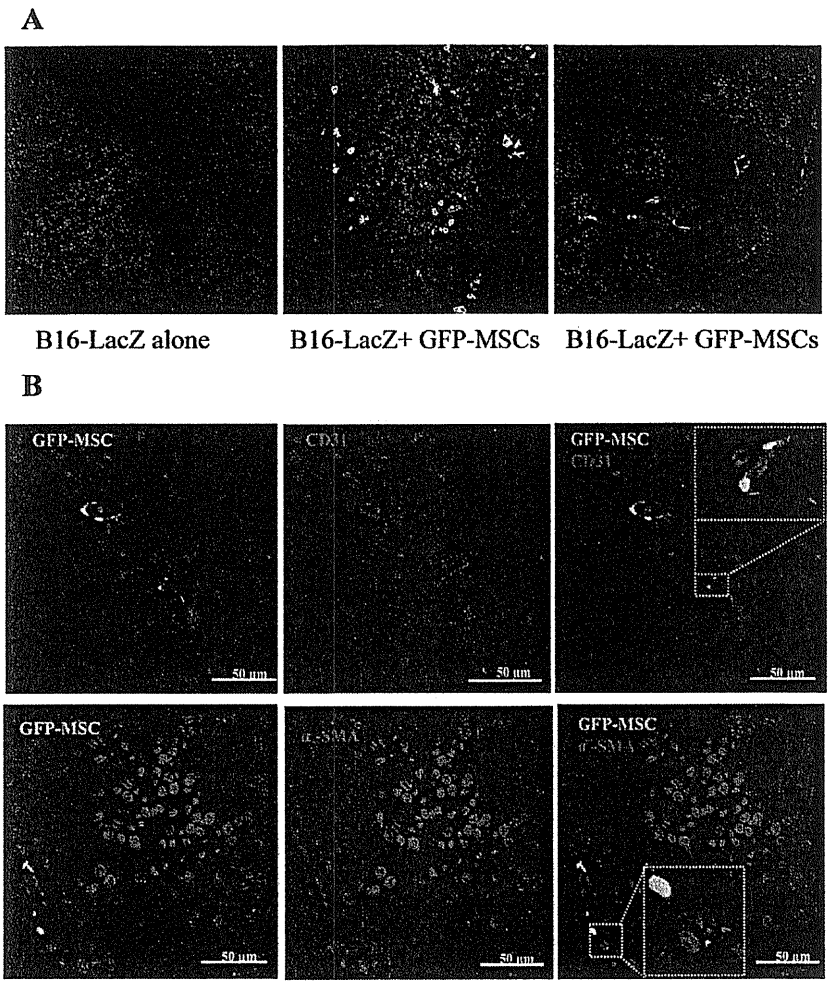


**Figure 6.** Presence and differentiation of MSCs in the tumors. (A) GFP-MSCs present and randomly distributed in the tumors on day 21 generated by co-injection of B16-LacZ cells and GFP-expressing MSCs. (B) GFP-MSCs closely localized to tumor vessels coexpressed the endothelial marker CD31, but did not coexpress the pericyte marker α-SMA.

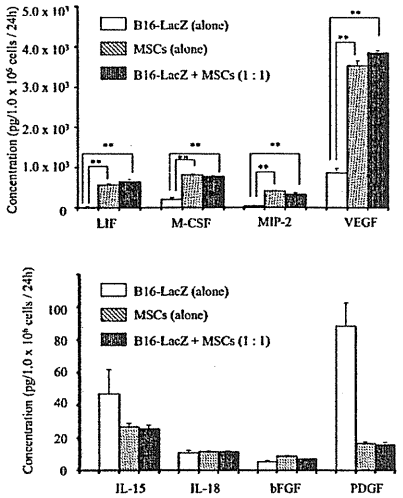


**Figure 7.** Expression of proangiogenic factors by MSCs. Secreted levels of LIF, M-CSF, MIP-2, VEGF (*upper panel*), IL-15, IL-18, bFGF and PDGF (*lower panel*) were analyzed in media from B16-LacZ cells ($1.0 \times 10^5$ cells/mL), MSCs ($1.0 \times 10^5$ cells/mL) or cocultures of B16-LacZ cells and MSCs ($1.0 \times 10^5$ cells/mL each). Concentrations were analyzed using a Luminex 200 ($n = 3$; $^{**}P < 0.01$).

### Differentiation of MSCs in the Tumors

To assess the role of MSCs in tumor promotion, MSCs from GFP mice (GFP-MSCs) were co-injected with B16-LacZ cells at a ratio of 1:1 into mice. Although GFP-MSCs presented in tumor tissues on day 21 (Figure 6A), the number of MSCs was quite low and MSCs were randomly distributed in tumor tissues. Some MSCs were closely presented at vessel structures. To assess differentiation and its association with tumor vessels, tumor tissues were stained with a CD31 antibody, as an endothelial marker (Figure 6B), or an_Q9α-SMA antibody, as a pericyte marker. Confocal microscopy revealed that some MSCs that were closely presented in the tumor vasculature expressed CD31 but not α-SMA.

### MSCs Secrete Several Angiogenic Cytokines

On the basis of the observation that MSCs promoted angiogenesis *in vivo*, we next assessed the levels of several secreted proangiogenic factors in media from MSCs and B16-LacZ cells. Levels of VEGF, MIP-2, M-CSF, LIF, IL-15, IL-18, bFGF, MIG and PDGF secreted by B16-LacZ cells ($1.0 \times 10^6$ cells) alone, MSCs ($1.0 \times 10^6$)Q3 alone and cocultures of B16-LacZ cells and MSCs ($1.0 \times 10^6$ cells each) were analyzed. Results from this analysis showed that MSCs secreted higher levels of LIF, M-CSF, MIP-2 and VEGF than tumor cells (Figure 7, *upper panel*). Both B16-LacZ cells and MSCs secreted little IL-15, IL-18, bFGF, MIG or PDGF (Figure 7, *lower panel*).

## DISCUSSION

In this study, we demonstrated that MSCs promote tumor cell proliferation *in vitro* and tumor growth *in vivo*. In both the presence and absence of direct contact, MSCs stimulated proliferation of B16-LacZ cells *in vitro*. Furthermore, combined administration of MSCs and tumor cells (B16-LacZ cells or LLCs) promoted tumor growth by enhancing angiogenesis in syngeneic tumor models.

This enhanced neovascularization can likely be attributed to direct support of neovascularization by MSCs and to secretion of angiogenic factors, including VEGF and others, by MSCs.

Our results suggest that both direct cell–cell contact and soluble factors likely play important roles in MSC-mediated stimulation of tumor cell proliferation *in vitro*, although we were not able to determine the molecules responsible for this phenotype. To date, few *in vitro* studies have assessed the effects of MSCs on tumor cell proliferation, because of the difficulty in distinguishing tumor cell proliferation from that of MSCs under coculture conditions. Sasser *et al.* (30) demonstrated that MSCs enhance proliferation of human breast cancer cells through the use of tumor cells that expressed stable red fluorescence. Similar to our β-galactosidase–based system, measurement of fluorescence intensity could distinguish between proliferation of fluorescent tumor cells and human MSCs in cocultures (30). Results from this study indicated that stimulation of tumor cell proliferation by human MSCs was solely due to secreted soluble factors, in contrast to our results suggesting that both direct contact and soluble factors play a role in stimulating proliferation. Another study demonstrated that treatment of pancreatic tumor cells with conditioned media from cancer-associated stromal fibroblasts enhanced cell proliferation *in vitro*; however, effects in cocultures containing both fibroblasts and tumor cells were not examined (4). Secreted IL-6 from fibroblasts was reported to enhance the rate of cancer cell proliferation in a previous study (5). Thus, IL-6 may represent one of the soluble factors partially responsible for stimulation of cell proliferation in B16-LacZ cells. Although these studies demonstrated MSC-mediated stimulation of tumor cell proliferation *in vitro*, none of them analyzed changes in the cell cycle. We did not observe any change of cell cycle distribution. This negative observation may have been because of using non-synchronized cells. Nevertheless, further investigation is needed to identify the precise molecules that mediate this effect.

Subcutaneous co-injection of tumor cells and MSCs resulted in more rapid tumor growth in mice compared with injection with tumor cells alone in assays using either B16-LacZ or LLC cells. Increased tumor growth was independent of the mouse strain background; indeed, similar effects were observed in both syngeneic mice and nude mice. The MSC cell line TSt-4 derived from fetal thymus tissue did not affect B16-LacZ tumors *in vivo*. The reported effects of MSCs on progression of primary tumors have been both pro- and antitumorigenic, but variability in these results, including ours, could be attributable to differences in the sources of the MSCs and the type of tumor model used for analysis. For example, intravenous injection of human MSCs into Kaposi's sarcoma-bearing nude mice inhibited tumor growth (26). MSCs also decreased proliferation of Kaposi's sarcoma cells *in vitro* under conditions of direct contact through inhibition of Akt signaling. Human MSCs were found to inhibit proliferation of a leukemia cell line and a small cell–lung cancer cell line *in vitro*, whereas tumor cells grew significantly faster when co-injected with MSCs into nonobese diabetic severe combined immunodeficient mice compared with injection of tumor cells alone (31). However, MSC-mediated inhibitory effects have only been observed in a few models, and most studies reported protumorigenic effects, consistent with our findings. Note also that immunosuppressive effects caused by MSCs were shown to promote B16 tumor growth in an allogeneic mouse model (32). However, this was not the case in our study, because we observed no difference in the effect of MSCs on tumor growth between nude and syngeneic mice.

We observed neither a change in the Ki-67 labeling index in the B16-LacZ + MSC tumors nor a high number of MSCs in the tumor tissues. These observations suggest that tumor promotion by MSCs was not due to stimulated tumor cell growth or an increased number of MSCs. We demonstrated that MSCs strongly stimulate tumor angiogenesis, likely through secretion of several angiogenic factors. The effects of MSCs on the tumor vasculature remain unclear and are likely to be complex (33,34). We hypothesize that MSCs exert paracrine effects on endothelial cells via secreted growth factors and cytokines, directly contributing to blood vessel formation in the tumor microenvironment. MSCs secrete many proangiogenic factors, including VEGF, IL-6, transforming growth factor-β and IL-8 (24,34–36), and secretion of these proangiogenic factors was shown to be significantly enhanced by treatment with conditioned media from tumor cells (24). However, we did not observe enhanced secretion of these factors from MSCs as a result of coculture with tumor cells, although MSCs did secrete higher amounts of proangiogenic factors than tumor cells. VEGF expression in MSCs can be enhanced by hypoxia, a common phenomenon in tumor tissues (37). Together, these data and our findings suggest that MSCs play a key role in tumor neovascularization.

Another contribution of MSCs to the tumor vasculature occurs through the support of vascular formation in tumor tissues. In the present study, we attempted to investigate the differentiation state of MSCs after co-injection with tumor cells using GFP-MSCs. Some MSCs closely presented to the tumor vasculature and expressed the endothelial cell marker CD31, but not the pericyte marker α-SMA. Grafted MSCs were shown to integrate into tumor vessel walls and express pericyte markers, but not endothelial markers, suggesting that MSCs in tumor tissues differentiate into pericytes and contribute to the tumor vasculature (25). Although this report was different from ours, these studies suggest that MSCs directly support the tumor vasculature by differentiating into endothelial cells, pericytes or other types of cells. Additionally, grafted MSCs were reported to differentiate into tumor-

associated fibroblasts and to contribute to tumor progression (38).

In conclusion, results from this study demonstrate that MSCs stimulate tumor cell proliferation *in vitro* and tumor growth *in vivo*. Enhanced tumor growth in syngeneic mouse models by MSCs may be, in part, due to promotion of tumor neovascularization by directly supporting the tumor vasculature and secreting proangiogenic factors. These results suggest that MSCs play an important role in tumor progression.

## ACKNOWLEDGMENTS

This work was supported in part by grants-in-aid for scientific research from the Ministry of Education, Science, Sports, Culture and Technology, Japan (numbers 16022206 and 20390229).

## DISCLOSURE

The authors declare that they have no competing interests as defined by *Molecular Medicine*, or other interests that might be perceived to influence the results and discussion reported in this paper.Q4

## REFERENCES


1. Dvorak HF. (1986). Tumors: wounds that do not heal. Similarities between tumor stroma generation and wound healing. *N. Engl. J. Med.* 315:1650–9.
2. Bissell MJ, Radisky D. (2001). Putting tumours in context. *Nat. Rev. Cancer.* 1:46–54.
3. Karnoub AE, *et al.* (2007). Mesenchymal stem cells within tumour stroma promote breast cancer metastasis. *Nature.* 449:557–63.
4. Hwang RF, *et al.* (2008). Cancer-associated stromal fibroblasts promote pancreatic tumor progression. *Cancer Res.* 68:918–26.
5. Studebaker AW, *et al.* (2008). Fibroblasts isolated from common sites of breast cancer metastasis enhance cancer cell growth rates and invasiveness in an interleukin-6-dependent manner. *Cancer Res.* 68:9087–95.
6. Kim S, *et al.* (2009). Carcinoma-produced factors activate myeloid cells through TLR2 to stimulate metastasis. *Nature.* 457:102–6.
7. Grugan KD, *et al.* (2010). Fibroblast-secreted hepatocyte growth factor plays a functional role in esophageal squamous cell carcinoma invasion. *Proc. Natl. Acad. Sci. U. S. A.* 107:11026–31.
8. Paulsson J, *et al.* (2009). Prognostic significance of stromal platelet-derived growth factor beta-receptor expression in human breast cancer. *Am. J. Pathol.* 175:334–41.
9. Utispan K, *et al.* (2010). Gene expression profiling of cholangiocarcinoma-derived fibroblast reveals alterations related to tumor progression and indicates periostin as a poor prognostic marker. *Mol. Cancer.* 9:13.
10. Wels J, Kaplan RN, Rafii S, Lyden D. (2008). Migratory neighbors and distant invaders: tumor-associated niche cells. *Genes. Dev.* 22:559–74.
11. Direkze NC, *et al.* (2004). Bone marrow contribution to tumor-associated myofibroblasts and fibroblasts. *Cancer Res.* 64:8492–5.
12. Udagawa T, Puder M, Wood M, Schaefer BC, D'Amato RJ. (2006). Analysis of tumor-associated stromal cells using SCID GFP transgenic mice: contribution of local and bone marrow-derived host cells. *FASEB J.* 20:95–102.
13. Worthley DL, *et al.* (2009). Human gastrointestinal neoplasia-associated myofibroblasts can develop from bone marrow-derived cells following allogeneic stem cell transplantation. *Stem Cells.* 27:1463–8.
14. Pittenger MF, et al. (1999). Multilineage potential of adult human mesenchymal stem cells. *Science.* 284:143–7.
15. Prockop DJ. (1997). Marrow stromal cells as stem cells for nonhematopoietic tissues. *Science.* 276:71–4.
16. Campagnoli C, *et al.* (2001). Identification of mesenchymal stem/progenitor cells in human first-trimester fetal blood, liver, and bone marrow. *Blood.* 98:2396–402.
17. Karp JM, Leng Teo GS. (2009). Mesenchymal stem cell homing: the devil is in the details. *Cell Stem Cell.* 4:206–16.
18. Ortiz LA, *et al.* (2003). Mesenchymal stem cell engraftment in lung is enhanced in response to bleomycin exposure and ameliorates its fibrotic effects. *Proc. Natl. Acad. Sci. U. S. A.* 100:8407–11.
19. Lian Q, *et al.* (2010). Functional mesenchymal stem cells derived from human induced pluripotent stem cells attenuate limb ischemia in mice. *Circulation.* 121:1113–23.
20. Studeny M, *et al.* (2004). Mesenchymal stem cells: potential precursors for tumor stroma and targeted-delivery vehicles for anticancer agent. *J. Natl. Cancer Inst.* 96:1593–603.
21. Kidd S, *et al.* (2009). Direct evidence of mesenchymal stem cell tropism for tumor and wounding microenvironments using in vivo bioluminescent imaging. *Stem Cells.* 27:2614–23.
22. Klopp AH, *et al.* (2007). Tumor irradiation increases the recruitment of circulating mesenchymal stem cells into the tumor microenvironment. *Cancer Res.* 67:11687–95.
23. Coffelt SB, *et al.* (2009). The pro-inflammatory peptide LL-37 promotes ovarian tumor progression through recruitment of multipotent mesenchymal stromal cells. *Proc. Natl. Acad. Sci. U. S. A.* 106:3806–11.
24. Spaeth EL, *et al.* (2009). Mesenchymal stem cell transition to tumor-associated fibroblasts contributes to fibrovascular network expansion and tumor progression. *PLoS One.* 4:e4992.
25. Bexell D, *et al.* (2009). Bone marrow multipotent mesenchymal stoma cells act as pericyte-like migratory vehicles in experimental gliomas. *Mol. Ther.* 17:183–90.
26. Khakoo AY, *et al.* (2006). Human mesenchymal stem cells exert potent antitumorigenic effects in a model of Kaposi's sarcoma. *J. Exp. Med.* 203:1235–47.
27. Watanabe Y, *et al.* (1992) A murine thymic stromal cell line which may support the differentiation of CD4–8- thymocytes into CD4+8- alpha beta T cell receptor positive T cells. *Cell. Immunol.* 142:385–97.
28. Umezawa A, *et al.* (1992). Multipotent marrow stromal cell line is able to induce hematopoiesis in vivo. *J. Cell Physiol.* 151:197–205.
29. Annabi B, *et al.* (2003). Hypoxia promotes murine bone-marrow-derived stromal cell migration and tube formation. *Stem Cells.* 21:337–47.
30. Sasser AK, *et al.* (2007). Human bone marrow stromal cells enhance breast cancer cell growth rates in a cell line-dependent manner when evaluated in 3D tumor environments. *Cancer Lett.* 254:255–64.
31. Ramasamy R, *et al.* (2007). Mesenchymal stem cells inhibit proliferation and apoptosis of tumor cells: impact on in vivo tumor growth. *Leukemia.* 21:304–10.
32. Djouad F, *et al.* (2003). Immunosuppressive effect of mesenchymal stem cells favors tumor growth in allogeneic animals. *Blood.* 102:3837–44.
33. Beckermann BM, *et al.* (2008). VEGF expression by mesenchymal stem cells contributes to angiogenesis in pancreatic carcinoma. *Br. J. Cancer.* 99:622–31.
34. Otsu K, *et al.* (2009). Concentration-dependent inhibition of angiogenesis by mesenchymal stem cells. *Blood.* 113:4197–205.
35. Gunn WG, *et al.* (2006). A crosstalk between myeloma cells and marrow stromal cells stimulates production of DKK1 and interleukin-6: a potential role in the development of lytic bone disease and tumor progression in multiple myeloma. *Stem Cells.* 24:986–91.
36. Romieu-Mourez R, *et al.* (2009). Cytokine modulation of TLR expression and activation in mesenchymal stromal cells leads to a proinflammatory phenotype. *J. Immunol.* 182:7963–73.
37. Potier E, *et al.* (2007). Hypoxia affects mesenchymal stromal cell osteogenic differentiation and angiogenic factor expression. *Bone.* 40:1078–87.
38. Mishra PJ, *et al.* (2008). Carcinoma-associated fibroblast-like differentiation of human mesenchymal stem cells. *Cancer Res.* 68:4331–9.

**Queries**

**Q1: Can CAG-EGFP be expanded?**

**Q2: Please expand GFP.**

**Q3: Should "1.0 x $10^6$" read "1.0 x $10^6$ cells"?**

**Q4: Please confirm that this disclosure statement is correct. If you do have something to declare, please provide that information.**

**Q5: Fig. 2: Please define OD595. Optical density absorbance at 595 nm?**

**Q6: Is a symbol such as the plus sign missing here?**

**Q7: Is this line correct as edited?**

**Q8: Please provide a new figure 1 with legible axes at a resolution of at least 300 dpi.**

**Q9: Is something missing here?**

# 新しい肺癌診療ガイドラインの考え方

弘前大学医学部循環器・呼吸器・腎臓内科助教 當麻景章
弘前大学医学部腫瘍内科教授 西條康夫

肺癌診療ガイドラインの改訂が2010年10月より順次行われている．日本肺癌学会ホームページ上で公開されており，非学会員でも閲覧・ダウンロードが可能である．現在，「集団検診」・「診断」と進行期「非小細胞肺癌」および「小細胞肺癌」の項目が公開されており，他の項目も順次公開予定である．前回改訂からの5年間で肺癌診療は大きく変わり，ガイドラインと実臨床に隔たりを生じていたが，今後はWeb上で更新が行われ，より早いアップデートがされていく見込みである．今回の改訂の特徴として，NCCNガイドラインと同じように病期別に治療選択樹形図が作成されていることが挙げられる．前回までは文章で推奨とエビデンスが細かく記述されていたが，樹形図とすることで，よりみやすく，容易に治療方法が選択でき，実臨床での使いやすさを考慮したものとなっている．

「集団検診」・「診断」の内容は前回から大きく変わるものはないが，診療ガイドラインは患者が対象であるのに対し，検診は健康人を対象としていることから，今回の改訂では，「集団検診」の項が独立した章として構成されることになった．

一方，治療内容に関しては，特にⅣ期未治療非小細胞肺癌において大きな改訂が行われている．まず，これまでは治療決定においてperformance status（PS）が重要な要素であったが，それに加えて上皮成長因子受容体（EGFR）遺伝子変異と組織型によって推奨される治療が示されている．これは，EGFR遺伝子変異がEGFR-TKIに対する効果予測因子として確立されたこと，非扁平上皮癌が治療対象となるベバシズマブ，ペメトレキセドが臨床導入されたことを反映している．特にEGFR遺伝子に関しては，検出検査が普及し，変異陽性患者が多い日本独自の特徴的なガイドラインとなった．また，非扁平上皮癌に対する治療に関しては，治療薬が増えて多くの改訂，進歩があったのに対し，扁平上皮癌の治療は前回と変わりなく，今後の新たな治療法の発見が望まれる．

初回治療に続けて行う維持療法に関しては，ペメトレキセドとエルロチニブの効果が海外の臨床試験で確認されているが，海外に比べて2次療法の実施率が高い日本での有益性が不透明な点から，今回は標準治療とされなかった．現在もいくつかの臨床試験が進行中であるが，わが国独自のエビデンスが待たれる．

PS 3，4の不良例は，これまで化学療法の適応でなかったが，今回はEGFR遺伝子変異陽性例に限りEGFR-TKIを考慮するようになった．ただし，PS不良はEGFR-TKIによる薬剤性肺障害のリスク因子であり，十分な管理と説明が必要である．

今回の改訂では，より患者を適切に層別化し，個別の治療を選択することが重要になっている．この傾向は今後も加速していくと考えられ，新たに発見されたEML4-ALK融合遺伝子に関しても，すでに検出方法，治療薬が開発され，近々，臨床導入される予定であるので，その結果を受けてガイドラインも改訂されると予想される．

Clinical Study

Oncology

Oncology 2011;81:84–90
DOI: 10.1159/000331681

Received: May 2, 2011
Accepted after revision: August 2, 2011
Published online: October 3, 2011

# Phase II Study of Irinotecan plus S-1 Combination for Previously Untreated Advanced Non-Small Cell Lung Cancer: Hokkaido Lung Cancer Clinical Study Group Trial (HOT) 0601

Kenji Akie[a] Satoshi Oizumi[b] Shigeaki Ogura[a] Naofumi Shinagawa[b] Eiki Kikuchi[b] Shinichi Fukumoto[c] Masao Harada[c] Ichiro Kinoshita[d] Tetsuya Kojima[e] Toshiyuki Harada[f] Yuka Fujita[g] Yoshinobu Ohsaki[h] Hirotoshi Dosaka-Akita[d] Hiroshi Isobe[e] Masaharu Nishimura[b] Hokkaido Lung Cancer Clinical Study Group

[a]Department of Respiratory Medicine, Sapporo City General Hospital, [b]First Department of Medicine, Hokkaido University School of Medicine, [c]Department of Respiratory Medicine, National Hospital Organization Hokkaido Cancer Center, [d]Department of Medical Oncology, Hokkaido University Graduate School of Medicine, [e]Department of Medical Oncology and Respiratory Medicine, KKR Sapporo Medical Center, and [f]Center for Respiratory Disease, Hokkaido Social Insurance Hospital, Sapporo, [g]Department of Respiratory Medicine, National Hospital Organization Asahikawa Medical Center, and [h]Respiratory Center, Asahikawa Medical University, Asahikawa, Japan

**Key Words**

Irinotecan · S-1 · Chemotherapy · Nonplatinum regimens · Non-small cell lung cancer, phase II

**Abstract**

***Objective:*** Platinum-free regimens can represent an alternative for advanced non-small cell lung cancer (NSCLC) if similar efficacy is provided with better tolerability. This study evaluated the efficacy and safety of combined irinotecan and S-1 for chemotherapy-naïve advanced NSCLC. ***Methods:*** Chemotherapy consisted of 4-week cycles of intravenous irinotecan (100 mg/m$^2$, days 1 and 15) and oral S-1 (80 mg/m$^2$, days 1–14). The primary endpoint was response rate, while secondary endpoints were overall survival, progression-free survival (PFS), and safety. ***Results:*** A total of 112 cycles was administered to 40 patients (median 3 cycles; range 1–6 cycles). Twelve patients showed partial response and 17 patients had stable disease, representing a response rate of 30% and a disease control rate of 72.5%. Median survival time and median PFS were 16.1 and 4.8 months, respectively. Hematological toxicities of grade 3 or 4 were neutropenia (32.5%) and anemia (5.0%). The most common nonhematological toxicities of grade 3 or 4 included diarrhea (15.0%) and anorexia (17.5%). Patients homo- or heterozygous for *UGTA1A*6* tended to show a higher incidence of grade 3 diarrhea ($p = 0.055$). ***Conclusion:*** The combination of irinotecan and S-1 offers good efficacy and tolerability for previously untreated advanced NSCLC. 

## Introduction

Platinum-based doublet chemotherapy was established in the 1990s, and it has become the standard first-line therapy for advanced non-small cell lung cancer (NSCLC) [1, 2]. Platinum compounds, particularly cis-

KARGER

Fax +41 61 306 12 34
E-Mail karger@karger.ch
www.karger.com


0030–2414/11/0812–0084$38.00/0

Accessible online at:
www.karger.com/ocl

Satoshi Oizumi
First Department of Medicine, Hokkaido University School of Medicine
North 15, West 7, Kita-ku
Sapporo 060-8638 (Japan)
Tel. +81 11 706 5911, E-Mail soizumi@med.hokudai.ac.jp

platin, are associated with considerable toxicity that may lead to reluctance on the part of both physicians and patients to initiate chemotherapy. Platinum-free regimens can offer a useful substitute if similar efficacy can be provided with reduced toxicity.

Third-generation agents are, in general, better tolerated than their first- and second-generation predecessors, and have shown single-agent activity. New anticancer drugs such as nucleoside analogs, vinca alkaloids, taxanes, camptothecin derivatives, and 5-fluorouracil derivatives provide alternatives to these platinum agents [3].

Among the new agents, irinotecan and S-1 have been developed in Japan. Irinotecan, a derivative of camptothecin, inhibits topoisomerase I and shows strong antitumor effects against NSCLC. Fukuoka et al. [4] reported that irinotecan monotherapy showed a 23% response rate (RR) with a median survival time (MST) of 42 weeks for previously untreated NSCLC. In addition, irinotecan plus cisplatin exhibited an RR of 52%, including 1 case of complete response (CR) with an MST of 44 weeks [5].

S-1 is a novel oral fluorouracil antitumor agent that consists of tegafur, 5-chloro-2,4-dihydroxypyridine (gimeracil, which inhibits dihydropyrimidine dehydrogenase) and potassium oxonate (oteracil potassium). In a phase II trial against metastatic NSCLC, S-1 showed a promising RR of 22% with an MST of 10.5 months [6]. S-1 combined with cisplatin or carboplatin exhibited promising efficacy with favorable toxicity profiles [7–11]. In addition, the LETS (Lung Cancer Evaluation of TS-1) study recently demonstrated that S-1 with carboplatin was noninferior in terms of overall survival (OS) compared with carboplatin and paclitaxel in patients with advanced NSCLC [12].

In preclinical models, optimal therapeutic synergy was observed with an irinotecan plus S-1 or 5-fluorouracil combination [13, 14]. The apoptosis rate of colon cancer cells increased after treatment with irinotecan plus 5-fluorouracil, corresponding to activation of Bax [13]. A potential mechanism of synergy between irinotecan plus S-1 was also suggested by the significant reduction in levels of thymidylate synthase [14].

Several studies of combination therapy with irinotecan plus S-1 have shown promising activity and safety, particularly for gastric or colorectal cancer [15, 16]. These findings led us to investigate the possibility of irinotecan combined with S-1 as a first-line regimen for NSCLC. This prospective phase II study evaluated the efficacy and safety of irinotecan plus S-1 therapy. As a supplemental study, associations between *UGT1A1* genotypes (**6* and **28*) and frequency of severe toxicity were also examined.

## Patients and Methods

*Patient Eligibility*

The ethics review boards at each participating institute approved this study, and each patient provided written informed consent prior to enrollment. Main eligibility criteria were: (1) histologically or cytologically confirmed NSCLC; (2) stage III disease without indication for curative irradiation, stage IV disease, or postoperative recurrence; (3) no prior chemotherapy; (4) measurable or assessable disease; (5) Eastern Cooperative Oncology Group (ECOG) performance status (PS) 0–2; (6) age between 20 and 75 years with white blood cell count $\geq$3,000/mm$^3$, hemoglobin $\geq$9.5 g/dl, platelet count $\geq$100,000/mm$^3$, total bilirubin $\leq$1.5 mg/dl, aspartate aminotransferase and alanine aminotransferase less than twice the upper limit of normal, creatinine $\leq$1.5 mg/dl, $P_aO_2$ $\geq$65 Torr or $SpO_2$ $\geq$92%, and (7) anticipated survival $\geq$3 months. Main exclusion criteria were: (1) serious concomitant systemic disorders including severe heart failure, uncontrollable angina, hypertension, diabetes mellitus, interstitial pneumonia, active infection, ulcer or another primary malignancy, (2) symptomatic brain metastases, (3) history of severe hypersensitivity, and (4) pregnancy.

*Treatment Schedule*

All patients received irinotecan (100 mg/m$^2$) on days 1 and 15. S-1 [40 mg for patients with body surface area (BSA) $\leq$1.25 m$^2$; 50 mg for patients with BSA >1.25 m$^2$ but $\leq$1.5 m$^2$, and 60 mg for patients with BSA $\geq$1.5 m$^2$] was administered twice daily for 2 weeks (days 1–14) followed by a 2-week pause. The treatment cycle was repeated every 4 weeks, and all patients received at least 4 cycles unless disease progressed, unacceptable toxicity occurred, the patient refused further treatment, or the physician decided to discontinue treatment. Second-line chemotherapy or other subsequent treatments were initiated at the discretion of the physician according to the protocol.

During the cycle, irinotecan was administered on day 15 when the patient met the following criteria: leukocyte count $\geq$2,000/mm$^3$, neutrophil count $\geq$1,000/mm$^3$, platelet count $\geq$50,000/mm$^3$, total bilirubin $\leq$1.5 mg/dl, no diarrhea or infection $\geq$grade 2, and no nonhematological toxicities $\geq$grade 3. S-1 was stopped for leukocyte count <2,000/mm$^3$, neutrophil count <1,000/mm$^3$, platelet count <50,000/mm$^3$, total bilirubin $\geq$1.5 mg/dl, infection or diarrhea $\geq$grade 2, or nonhematological toxicities $\geq$grade 3.

Subsequent cycles were delayed until recovery for leukocyte count <3,000/mm$^3$, neutrophil count <1,500/mm$^3$, platelet count <100,000/mm$^3$, total bilirubin $\geq$1.5 mg/dl, any infection or diarrhea, PS worsened to $\geq$PS 3, or any nonhematological toxicities $\geq$grade 3.

Dose reductions of both agents were made in subsequent cycles for grade 4 neutropenia lasting $\geq$4 days, febrile neutropenia, thrombocytopenia <20,000/mm$^3$, or nonhematological toxicities $\geq$grade 3 except for anorexia, nausea, and vomiting. The dose of either S-1 or irinotecan alone was reduced for the next course when S-1 was stopped longer than 4 days or irinotecan had not been administered on day 15 in the previous cycle. When the patient experienced adverse events even after the first reduction, no second reduction was permitted and the protocol treatment was terminated.

*Treatment Assessment*

Physical examination, determination of PS, laboratory tests, and chest radiography were performed at baseline and repeated at least every 2 weeks during treatment. Tumor responses were assessed using chest radiography, computed tomography, or magnetic resonance imaging (when clinically indicated) before and during treatment and repeated at least every month until progression. Responses were classified as CR, partial response (PR), stable disease (SD), progressive disease or nonevaluable on the basis of Response Evaluation Criteria in Solid Tumors (RECIST) 1.0 [17]. Disease control rate was defined as the sum of the objective response (CR or PR) rate plus the rate of SD. Progression was defined as progressive disease according to RECIST 1.0, clinical progression as judged by the investigator, or death from any cause without progression. Clinical response data were all confirmed by a central review.

Progression-free survival (PFS) was counted from the date of enrollment to the date on which progressive disease was first confirmed by the assessment of the investigator. OS was calculated from the date of enrollment to the date of death or confirmation of survival. For patients without any events, data were censored on the last date with nonevent status. The National Cancer Institute Common Toxicity Criteria (NCI-CTC) version 3.0 were used to grade adverse events.

*Study Endpoints and Statistical Considerations*

The primary endpoint was overall response rate (ORR). Sample size was calculated as 36 in total to confirm an RR of 40% as a desirable target level and RR of 20% as uninteresting with an alpha error of 0.05 and a power of 0.8. Allowing for a patient ineligibility rate of 10%, we initially planned to enroll 40 patients. Secondary endpoints were PFS, OS, and toxicity profiles. Survival outcomes were estimated using the Kaplan-Meier method.

*UGT1A1 Analyses*

All *UGT1A1* analyses were performed at the Biomedical Laboratories (Tokyo, Japan) using the Invader assay. Briefly, DNA was extracted from peripheral blood samples according to instructions from the manufacturer. The invader assay detects *UGT1A1* genotypes by use of the cleavase enzyme and a fluorescence resonance energy transfer cassette. Probes were designed for detecting the genotypes associated with *UGT1A1**6 and *28. The *UGT1A1**6 target site is 211G/A in exon 1, and *UGT1A1**28 has 7 TA repeats within the TATA box, as previously reported [18, 19].

## Results

*Patient Characteristics*

Forty patients (28 men, 12 women) from 8 institutions were enrolled in this study from August 2006 to July 2008. Patient characteristics are outlined in table 1. Median age at the time of entry to the study was 64 years (range 42–75 years). ECOG PS was 0 in 23 patients (57.5%), and 32 patients (80.0%) had stage IV disease. In addition, 29 patients (72.5%) had adenocarcinoma, and 8 (20.0%) had squamous cell carcinoma.

**Table 1.** Patient characteristics

| Characteristics | n | % |
|---|---|---|
| Age, years | | |
| Median | 64 | |
| Range | 42–75 | |
| Sex | | |
| Male | 28 | 70.0 |
| Female | 12 | 30.0 |
| ECOG PS | | |
| 0 | 23 | 57.5 |
| 1 | 17 | 42.5 |
| Disease stage | | |
| IIIB | 6 | 15.0 |
| IV | 32 | 80.0 |
| Recurrence after surgery | 2 | 5.0 |
| Histology | | |
| Adenocarcinoma | 29 | 72.5 |
| Squamous cell carcinoma | 8 | 20.0 |
| Unclassified NSCLC | 3 | 7.5 |

**Table 2.** Reason for discontinuation of protocol treatment

| | Cycle 1 | Cycle 2 | Cycle 3 | Total |
|---|---|---|---|---|
| Disease progression | 4 | 3 | 2 | 9 |
| Unacceptable toxicity | 4 | 6 | 2 | 12 |

*Response to Therapy and Survival*

The 40 patients received a total of 112 cycles (median 3 cycles; range 1–6 cycles), with 19 patients (47.5%) completing ≥4 cycles. The dose of agents was reduced in 14 patients (35%) because of toxicities, and protocol treatment was terminated in 21 patients (52.5%) before completion of 4 cycles. Of the 21 patients, treatment was discontinued in 9 patients because of disease progression and in 12 patients who experienced unacceptable toxicity (table 2). Mean relative dose intensities of S-1 and irinotecan were 95% each. Subsequently, 38 patients were assessable for tumor responses. Twelve patients exhibited PR, and 17 patients exhibited SD, resulting in an RR of 30% [95% confidence interval (CI), 16.6–46.5%] and a disease control rate of 72.5% (95% CI, 56.1–85.4%; table 3). The lower end of the 95% CI was thus lower than the threshold ORR of 20%, and the primary endpoint was not met. Disease progressed in 9 cases. The final survival assessment was carried out in March 2010 (>1 year after the last patient enrollment). With a median follow-up time of 16.1 months, MST and median PFS for all en-